Electronic Supplementary Material (ESI) for Journal of Materials Chemistry C.

Shape- and excitation-dependent charge-carrier dynamics in colloidal MAPbI perovskites as nanostripes, nanosheets and nanoplatelets

Eugen Klein,[1] Chris Rehhagen,[1] Rostyslav Lesyuk,[1,2] Christian Klinke[1,3,4]*

[1] *Institute of Physics, University of Rostock, Albert-Einstein-Strasse 23, 18059 Rostock, Germany*
[2] *Pidstryhach Institute for applied problems of mechanics and mathematics of NAS of Ukraine, Naukowa str. 3b, 79060 Lviv, Ukraine*
[3] *Department "Life, Light & Matter", University of Rostock, Albert-Einstein-Strasse 25, 18059 Rostock, Germany*
[4] *Department of Chemistry, Swansea University – Singleton Park, Swansea SA2 8PP, United Kingdom*
* Corresponding author: christian.klinke@uni-rostock.de

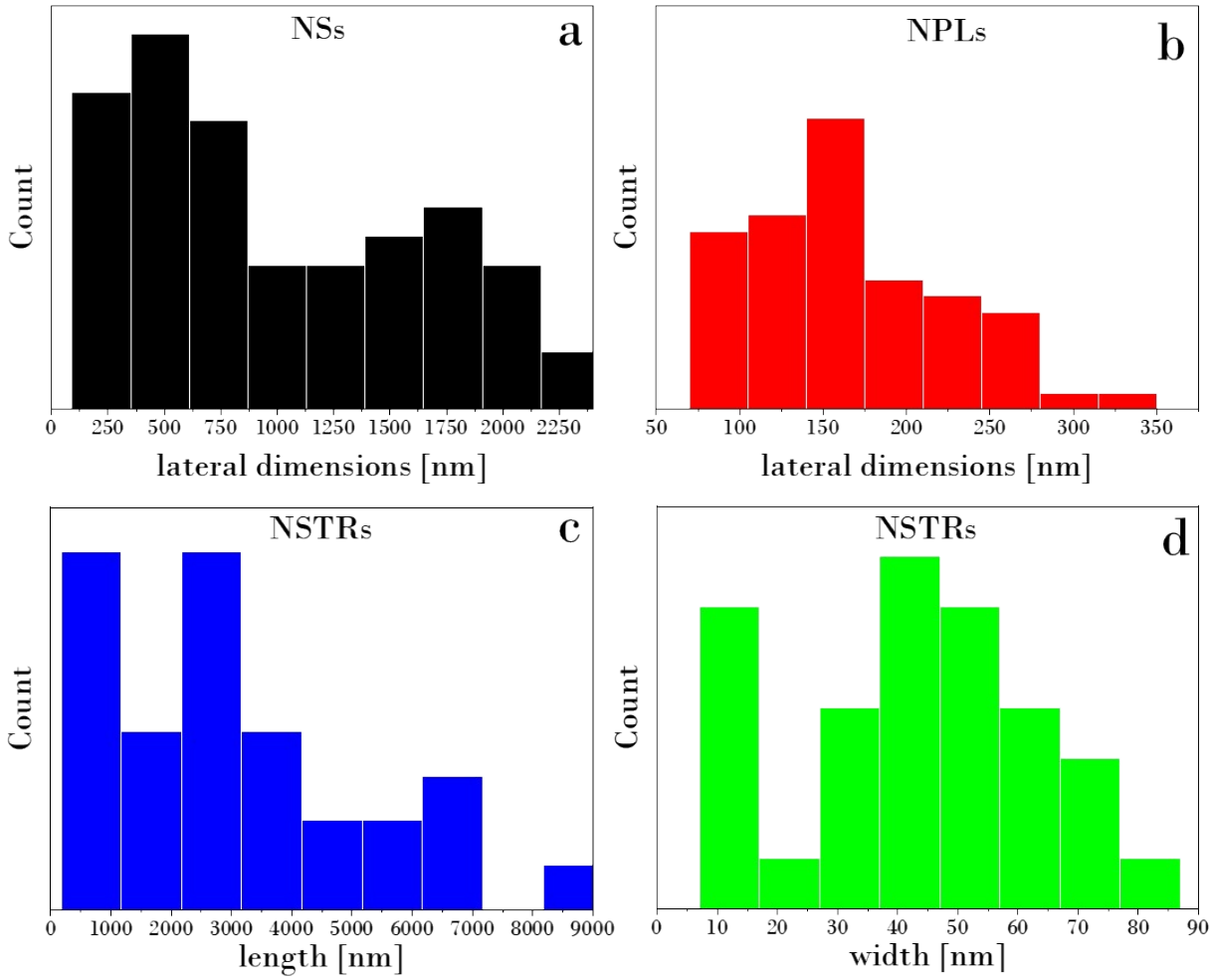

Figure S1. Polydispersity of the lateral dimensions of (a) nanosheets, (b) nanoplatelets and (c+d) nanostripes.

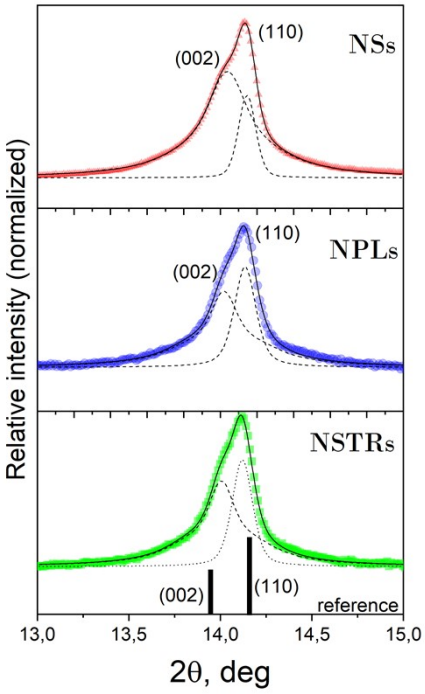

Figure S2. XRD reflection at 14° for the three types of nanomaterials. (002) and (110) reflections can be resolved by a numerical fitting with pseudo-Voigt function and the lattice constants $a=b$ and c can be calculated as 8.85 and 12.64 Å respectively. (002) reflection is more broadened than (110) and is attributed to the thickness direction.

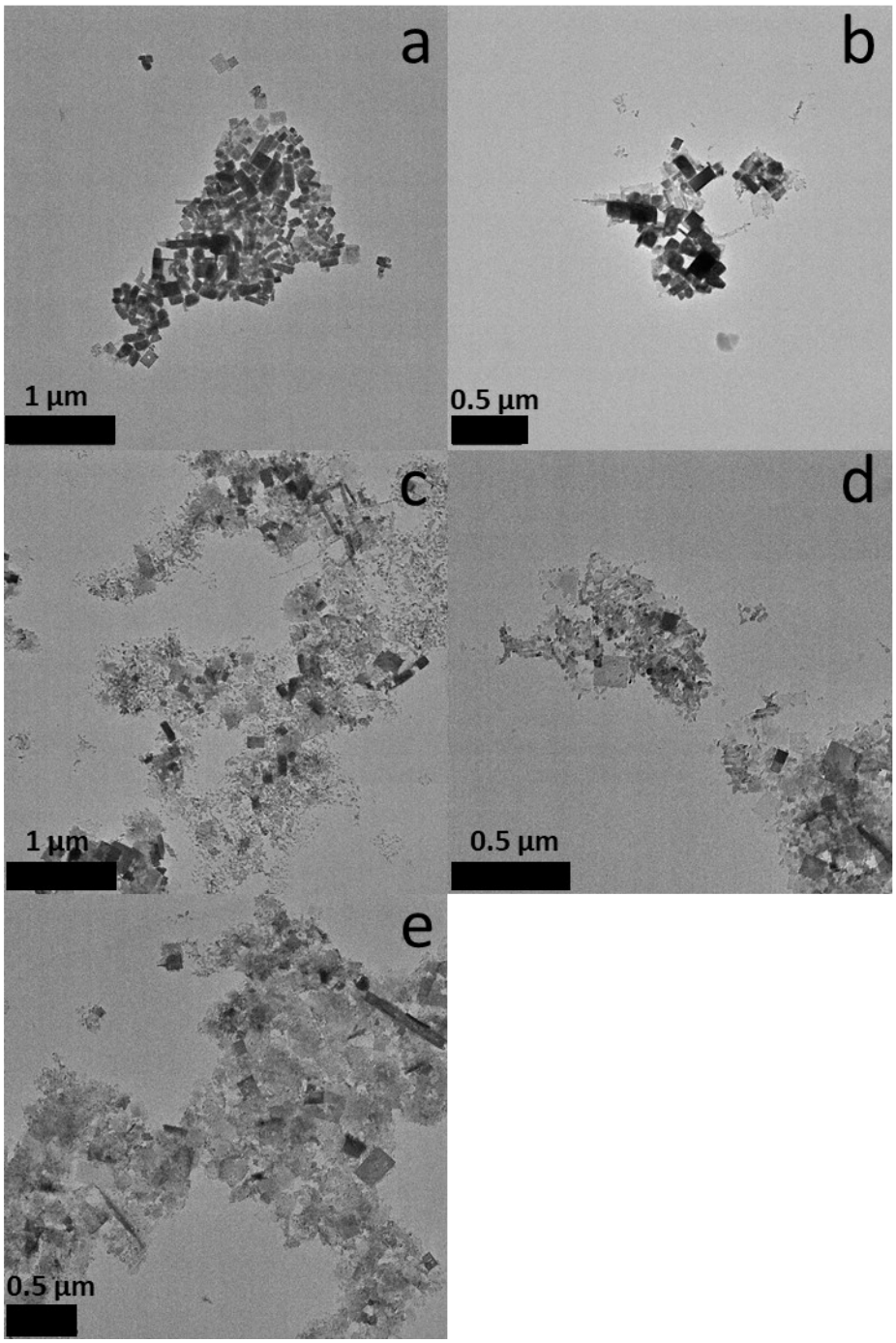

Figure S3. BF-TEM images of MAPbI nanoparticles prepared with a different amount of DPE, (a) 8 mL, (b) 10 mL (c) 12 mL, (d) 15 mL, (e) 20 mL.

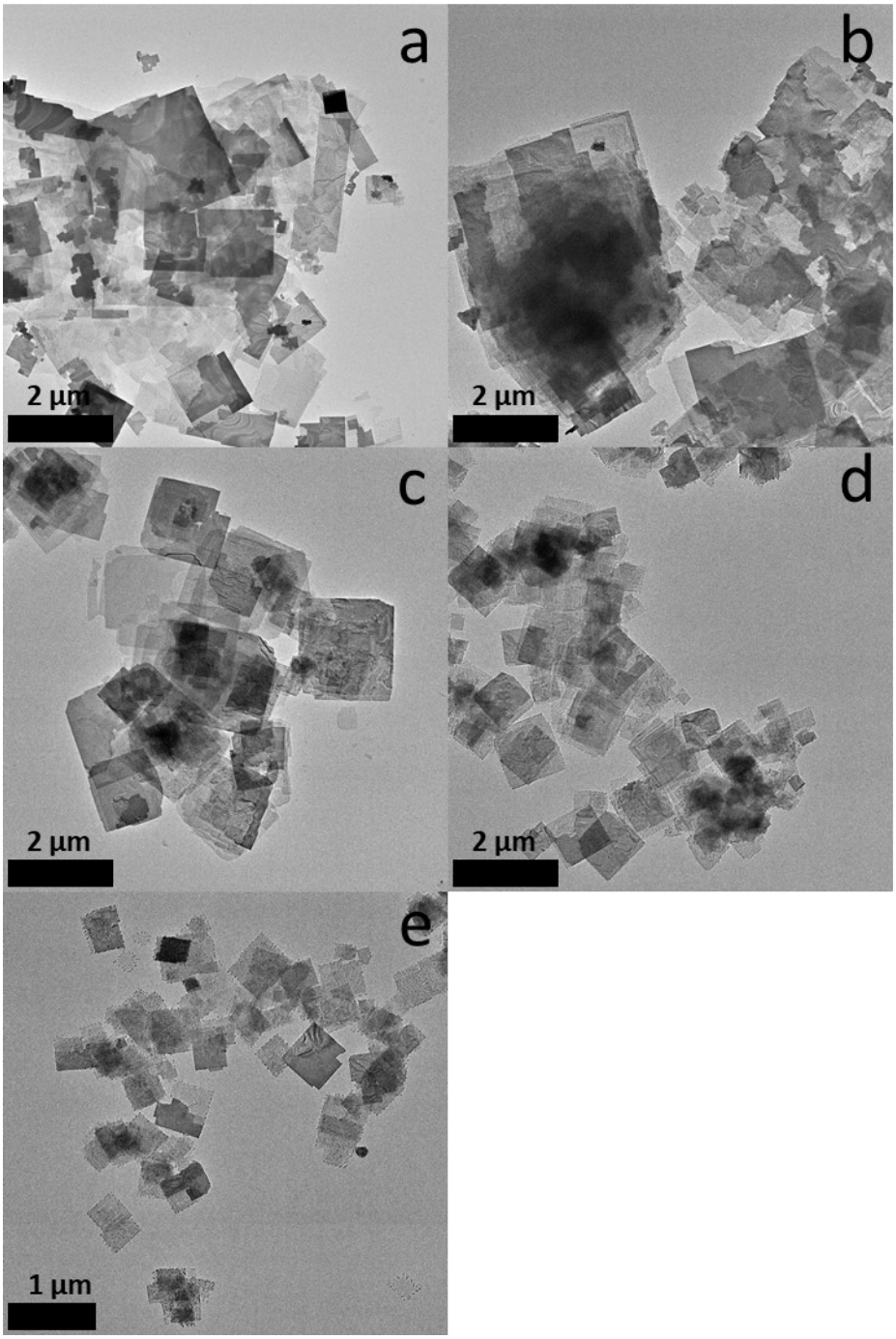

Figure S4. BF-TEM images of MAPbI nanoparticles prepared with a different method and less amounts of DPE, (a) 6 mL, (b) 8 mL (c) 10 mL, (d) 12 mL, (e) 14 mL.

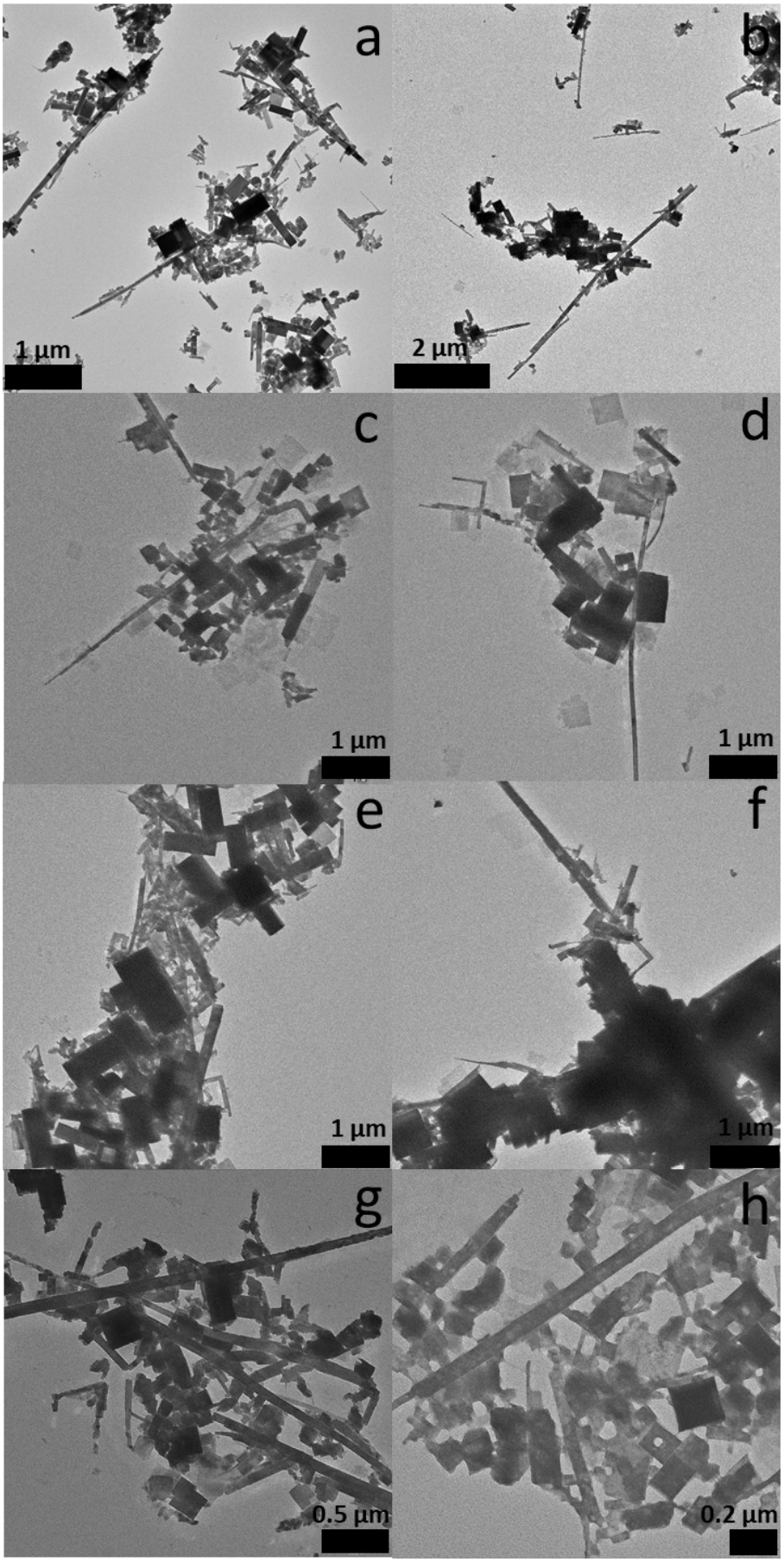

Figure S5. BF-TEM images of MAPbI nanoparticles prepared at (a) 88 °C, (b) 92 °C, (c) a lower amount (0.38 mL) of HDA, (d) a higher amount (0.5 mL) of HDA, (e) a lower amount (0.06 mL) of MAI, (f) a higher amount (0.07 mL) of MAI, (g) 0.23 mL dodecylamine, (h) 0.3 mL of tetradecylamine.

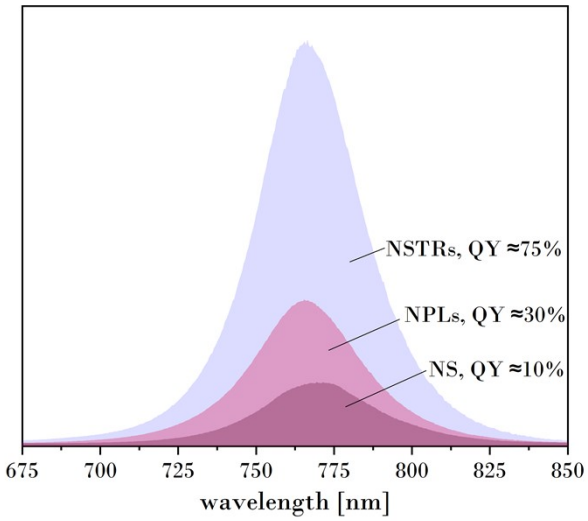

Figure S6. Photoluminescence of the samples of NSs, NPLs and NSTRs in solution (in toluene) during the PLQY measurements in integration sphere SC-30 (Edinburgh).

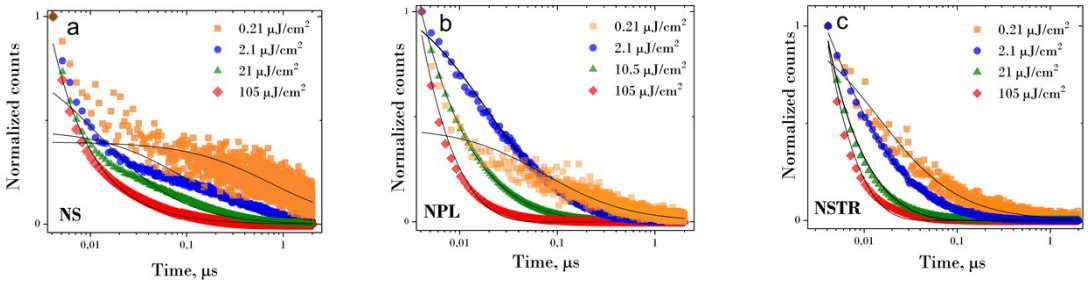

Figure S7. Fitting of decay traces with analytical solution of the rate equation with monomolecular and bimolecular rates. With growing excitation, the fitting improves reaching a maximum at ~10–20 μJ/cm² fluences. Decays at the largest excitation fluence of 105 μJ/cm² cannot be fitted well – possibly due to involved three-body processes.

It assumed the combination of monomolecular and bimolecular processes according to rate equation:

$$\frac{dn}{dt} = -k_1 n - \gamma n^2 \qquad (1),$$

where k_1 and γ are decay rates of monomolecular and bimolecular recombination, n is the concentration of charge carriers in the material at the time t.

Analytical solution of the equation (1):

$$n(t) = \frac{n(0) \cdot exp(-\frac{t}{\tau})}{1 + \gamma\tau \cdot n(0)\left(1 - exp\left(-\frac{t}{\tau}\right)\right)} \qquad (2),$$

$n(0)$ – concentration of charge carriers at time t=0 directly after the excitation pulse, γ – rate of the bimolecular process (in particular, EEA), τ – intrinsic lifetime of charge carriers (excitons). The fits are performed without any constraints using OriginPro2018b. The detailed analysis of the EEA model is addressed to further studies.

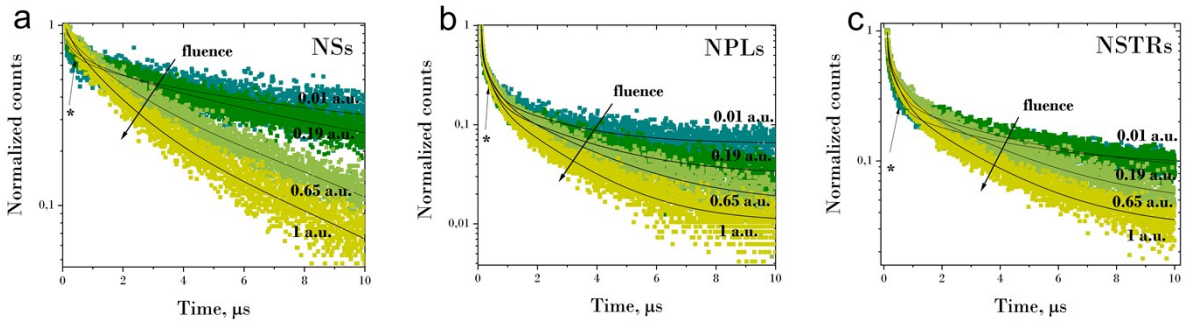

Figure S8. PL decays of NSs, NPLs and NSTRs in ensembles (colloidal solution) showing prolonged times in comparison to FLIM measurements. Three-exponential fits are plotted as black lines. Asterix shows the short components which substantially contributes at low excitation fluences. 1 a.u. roughly corresponds to the energy density of 0.004 μJ/cm^2 per pulse and is nearly 2 orders of magnitude smaller than the lowest excitation fluence in FLIM configuration.

The excitation of the laser (375 nm) in the low-excitation mode largely influences the decay due to the second order diffraction of the stray light (750 nm, close to the PL maximum), so the first three nanoseconds of the decay were eliminated for all the excitations and tail-fitting procedure was performed.

	FLIM											
	Fluence	t_1	A_1	t_2	A_2	t_3	A_3	<t>	f_1	f_2	f_3	<rate>
	μJ/cm²	μs		μs		μs		μs				1/μs
NS	0.210	0.0025	2.07	0.0309	0.33	1.1557	0.25	1.10	0.02	0.03	0.95	0.91
	2.105	0.0068	1.06	0.1433	0.11	0.6531	0.16	0.55	0.06	0.12	0.82	1.80
	21.045	0.0060	1.13	0.1024	0.18	0.3905	0.07	0.23	0.13	0.37	0.50	4.28
	105.226	0.0053	1.43	0.0589	0.16	0.2547	0.02	0.09	0.33	0.40	0.27	10.67
NPL	0.210	0.0049	1.33	0.0680	0.12	0.3973	0.17	0.33	0.08	0.10	0.82	3.02
	2.105	0.0068	0.71	0.0484	0.48	0.2200	0.15	0.14	0.08	0.38	0.54	7.31
	21.045	0.0047	1.69	0.0370	0.01	0.2600	0.01	0.05	0.77	0.04	0.19	18.47
	105.226	0.0030	3.10	0.0223	0.16	0.1554	0.01	0.02	0.66	0.25	0.09	48.09
NSTR	0.210	0.0052	1.03	0.0390	0.40	0.2955	0.13	0.20	0.09	0.26	0.65	4.94
	2.105	0.0060	1.19	0.0287	0.55	0.1493	0.11	0.07	0.18	0.41	0.41	13.53
	21.045	0.0044	2.32	0.0234	0.26	0.1171	0.02	0.02	0.55	0.33	0.12	40.75
	105.226	0.0022	5.01	0.0147	0.23	0.0819	0.01	0.01	0.73	0.22	0.05	109.09
	Ensemble measurement											
	Fluence	t_1	A_1	t_2	A_2	t_3	A_3	<t>	f_1	f_2	f_3	<rate>
	μJ/cm²	μs		μs		μs		μs				1/μs
NSs	0.082	0.2643	0.28	1.6775	0.16	9.7898	0.46	9.20	0.02	0.06	0.93	0.11
	0.188	0.2643	0.17	1.6775	0.17	9.7898	0.49	9.26	0.01	0.06	0.94	0.11
	0.305	0.2643	0.08	1.6775	0.27	9.7898	0.59	9.17	0.00	0.07	0.92	0.11
	0.475	0.2643	0.06	1.6775	0.39	9.7898	0.55	8.89	0.00	0.11	0.89	0.11
	0.648	0.2643	0.10	1.6775	0.46	9.7898	0.48	8.60	0.00	0.14	0.85	0.12
	1.000	0.2643	0.21	1.6775	0.61	9.7898	0.30	7.61	0.01	0.25	0.73	0.13
NPLs	0.082	0.0286	25.22	0.2940	0.47	2.3110	0.13	0.64	0.63	0.12	0.25	1.56
	0.188	0.0286	24.52	0.2940	0.44	2.3110	0.16	0.75	0.59	0.11	0.30	1.33
	0.305	0.0286	26.93	0.2940	0.45	2.3110	0.18	0.78	0.58	0.10	0.32	1.29
	0.475	0.0286	26.77	0.2940	0.49	2.3110	0.22	0.87	0.54	0.10	0.36	1.15
	0.648	0.0286	28.24	0.2940	0.49	2.3110	0.49	1.28	0.39	0.07	0.54	0.78
	1.000	0.0286	27.99	0.2940	0.58	2.3110	0.16	0.68	0.60	0.13	0.27	1.47
NSTRs	0.082	0.0348	28.99	0.3501	0.56	2.5871	0.21	0.85	0.58	0.11	0.31	1.17
	0.188	0.0348	15.58	0.3501	0.46	2.5871	0.21	1.19	0.43	0.13	0.44	0.84
	0.305	0.0348	11.05	0.3501	0.42	2.5871	0.23	1.42	0.34	0.13	0.53	0.70
	0.475	0.0348	5.14	0.3501	0.42	2.5871	0.27	1.83	0.17	0.14	0.68	0.55
	0.648	0.0348	3.13	0.3501	0.40	2.5871	0.28	1.98	0.11	0.14	0.74	0.50
	1.000	0.0348	9.54	0.3501	0.49	2.5871	0.27	1.57	0.27	0.14	0.58	0.64

Table S1. Fitting parameters for the fits presented in Figures 3, S5

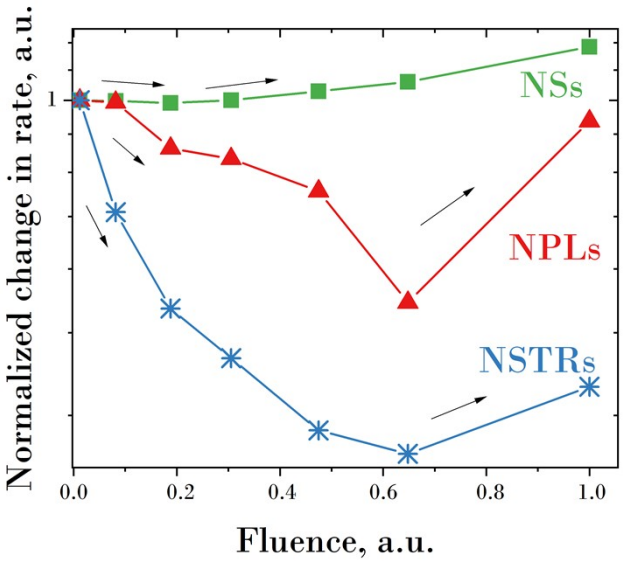

Figure S9. Normalized intensity-weighted decay rates in ensemble measurements for nanosheets, nanoplatelets, and nanostripes showing the trends with growing excitation fluence.

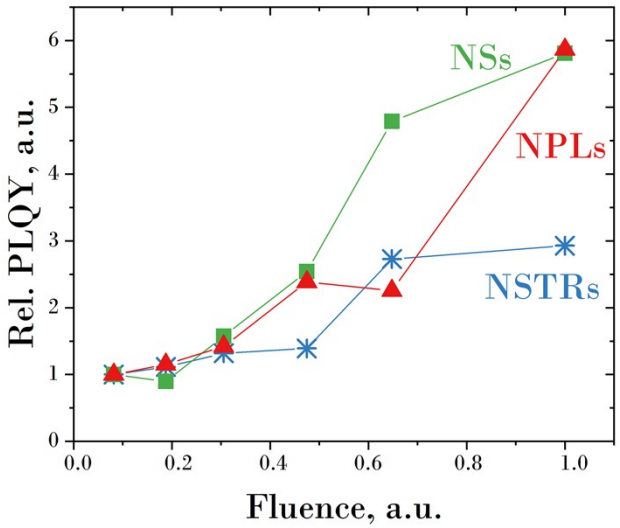

Figure S10. Relative QY in the ensemble measurements for nanosheets, nanoplatelets, and nanostripes.

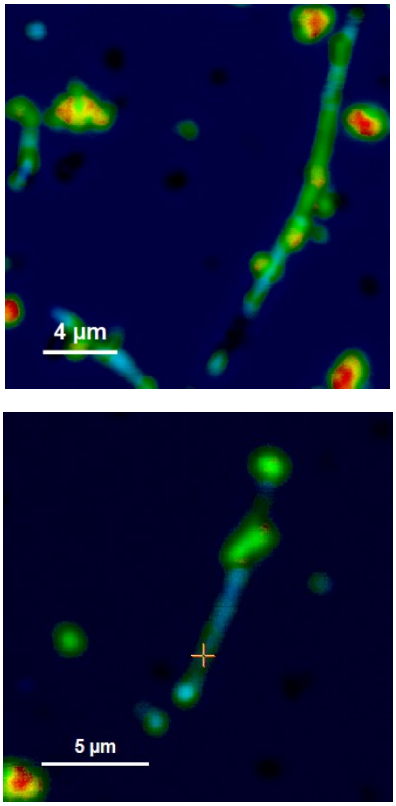

Figure S11. NSTRs in the fluorescence microscope MT200 (FLIM). Next to the NSTR few NPLs can be observed.

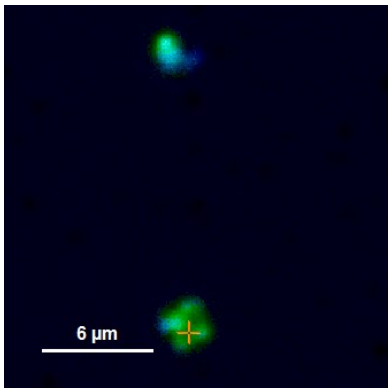

Figure S12. Image of a NS taken by scanning in the fluorescence microscope (FLIM).